ELSEVIER

Mechanisms of Development 121 (2004) 659–671

www.elsevier.com/locate/modo

Research paper

Mutations affecting somite formation in the Medaka (*Oryzias latipes*)

Harun Elmasri[a,1], Christoph Winkler[a,*,1], Daniel Liedtke[a], Takao Sasado[b], Chikako Morinaga[b], Hiroshi Suwa[b], Katsutoshi Niwa[b], Thorsten Henrich[b], Yukihiro Hirose[c], Akihito Yasuoka[d], Hiroki Yoda[e], Tomomi Watanabe[f], Tomonori Deguchi[e], Norihisa Iwanami[g], Sanae Kunimatsu[g], Masakazu Osakada[h], Felix Loosli[i], Rebecca Quiring[i], Matthias Carl[i], Clemens Grabher[i], Sylke Winkler[i], Filippo Del Bene[i], Joachim Wittbrodt[i], Keiko Abe[d], Yousuke Takahama[g], Katsuhito Takahashi[h], Toshiaki Katada[f], Hiroshi Nishina[f], Hisato Kondoh[b,e], Makoto Furutani-Seiki[b,*]

[a]*Department of Physiological Chemistry I, Biocenter, University of Wuerzburg, Am Hubland D-97074 Wuerzburg, Germany*
[b]*ERATO, Kondoh Differentiation Signaling Project, Japan Science and Technology Agency, Kyoto 606-8305, Japan*
[c]*Graduate School of Biostudies, Kyoto University, Kyoto 606-8501, Japan*
[d]*Department of Applied Biological Chemistry, University of Tokyo, Tokyo 113-0033, Japan*
[e]*Graduate School of Frontier Biosciences, Osaka University, Osaka 565-0871, Japan*
[f]*Department of Physiological Chemistry, Graduate School of Pharmaceutical Sciences, University of Tokyo, Tokyo 113-0033, Japan*
[g]*Division of Experimental Immunology, Institute for Genome Research, The University of Tokushima, Tokushima 770-8503, Japan*
[h]*Department of Molecular Medicine & Pathophysiology, Research Institute, Osaka Medical Center for Cancer and Cardiovascular Diseases, Osaka 537-8511, Japan*
[i]*Developmental Biology Programme, EMBL Heidelberg, Meyerhofstrasse 1, D-69117, Heidelberg, Germany*

Received 31 January 2004; received in revised form 21 March 2004; accepted 3 April 2004

Abstract

The metameric structure of the vertebrate trunk is generated by repeated formation of somites from the unsegmented presomitic mesoderm (PSM). We report the initial characterization of nine different mutants affecting segmentation that were isolated in a large-scale mutagenesis screen in Medaka (*Oryzias latipes*). Four mutants were identified that show a complete or partial absence of somites or somite boundaries. In addition, five mutations were found that cause fused somites or somites with irregular sizes and shapes. In situ hybridization analysis using specific markers involved in the segmentation clock and antero-posterior (A-P) polarity of somites revealed that the nine mutants can be compiled into two groups. In group 1, mutants exhibit defects in tailbud formation and PSM prepatterning, whereas A-P identity in the somites is defective in group 2 mutants. Three mutants (*planlos*, *pll*; *schnelles ende, sne*; *samidare*, *sam*) have characteristic phenotypes that are similar to those in zebrafish mutants affected in the Delta/Notch signaling pathway. The majority of mutants, however, exhibit somitic phenotypes distinct from those found in zebrafish, such as individually fused somites and irregular somite sizes. Thus, these Medaka mutants can be expected to provide clues to uncovering novel components essential for somitogenesis.

Keywords: *Oryzias latipes*; Somites; Segmentation clock; Oscillator; Delta/Notch

1. Introduction

Segmentation in vertebrates is most evident by the metameric appearance of somites during embryogenesis. Somites are transient structures in the paraxial mesoderm that develop into muscle, axial skeleton and dermis during later development. They form sequentially by recurrent separation from the unsegmented presomitic mesoderm (PSM), a growth zone at the caudal end of the embryo. Their formation shows a tightly regulated temporal periodicity that is controlled by a molecular oscillator, the segmentation clock.

Over the last years, several models have been postulated to explain the regular and repeated appearance of somites

* Corresponding authors. Tel.: +49-931-888-4142; fax: +49-931-888-4150.
E-mail addresses: cwinkler@biozentrum.uni-wuerzburg.de (C. Winkler); furutaniseiki@dsp.jst.go.jp (M. Furutani-Seiki).
[1] Contributed equally.

0925-4773/$ - see front matter © 2004 Elsevier Ireland Ltd. All rights reserved.
doi:10.1016/j.mod.2004.04.003

(reviewed in Pourquie, 2001, 2003; Saga and Takeda, 2001). These are based on the initial observation in chicken that the basic helix–loop–helix (bHLH) gene *c-hairy1* shows cyclic expression in the PSM. Its transcription starts at the caudal end of the tailbud and then sweeps the PSM in a caudal to rostral direction. As this wave reaches the anterior end of the unsegmented PSM, a new pair of epithelialized somites buds off from the PSM and the next cycle of somite formation begins. The formation of each pair of somites can be subdivided into three steps (see Pourquie, 2001). First, precursor cells in the posterior PSM exit their undetermined state and receive a prepattern. As the growth zone extends caudally, these cells will be positioned in the anterior part of the PSM where they undergo maturation. They will form somitomeres that acquire an A-P polarity. Finally, these somitomeres become epithelialized and bud off from the PSM.

Besides *c-hairy1*, several other components of the Delta/Notch signaling pathway have later been shown to synchronously oscillate in the PSM. A molecular oscillator, the segmentation clock, has then been postulated that controls cyclic expression in the PSM and the repeated appearance of somites. The exact molecular nature of this oscillator remains unknown, although experiments in mice, chicken and zebrafish over the last years have clearly demonstrated that the Delta/Notch pathway plays crucial roles in this process (reviewed by Saga and Takeda, 2001; Pourquie, 2003). Interference with components of this pathway results in the block of oscillating gene expression and consequently impaired somite formation (Jouve et al., 2000; Leimeister et al., 2000; Serth et al., 2003). Recently, three additional pathways have been implicated in somitogenesis. Experiments in mouse have demonstrated that the Wnt signaling inhibitor *Axin2* shows cyclic expression in the PSM even if Delta/Notch signaling is impaired (Aulehla et al., 2003). In this report, it was postulated that Wnt3a acts as upstream regulator of oscillating Notch activity, as *Wnt3a* knock-out mice lack cyclic expression of both *Axin2* and *Lunatic fringe*, a component of the Delta/Notch pathway. Furthermore, molecular analysis of the zebrafish *fused somites* (*fss*) mutant identified the T-box gene *tbx24* (Nikaido et al., 2002). Its activity contributes to the generation of a 'wavefront' that stabilizes oscillating Notch activity in the anterior PSM at the location where the next somite will form. Finally, experiments in zebrafish and chicken have shown that FGF signaling participates in somite formation (Sawada et al., 2001; Dubrulle et al., 2001). It was shown that certain threshold levels of FGF8 antagonize the Tbx24 wavefront activity. Therefore, graded FGF signaling provides positional information in the PSM and thereby regulates the establishment of new somite boundaries at correct positions (reviewed in Holley and Takeda, 2002).

Mutant analysis in zebrafish has provided important insights into the dynamics of gene regulation during somite formation. The molecular identification of the *after eight* (*deltaD*; Holley et al., 2000), *deadly seven* (*notch1*; Holley et al., 2002) and *white tail/mindbomb* (*mib*; Itoh et al., 2003) mutants confirmed the importance of the Delta/Notch pathway for somitogenesis. Also, analysis of a deletion mutant for the Delta/Notch targets *her1* (*hairy/enhancer of split related-1*) and *her7* suggested that these genes are required for prepatterning the zebrafish PSM (Henry et al., 2002). However, several aspects of somite formation remain unclear. Although Delta/Notch, FGF and Wnt signaling pathways clearly play important roles in this process, their interactions at the molecular level are not understood. Also, the apparently different regulation of formation of anterior in comparison to posterior somites, with genetic redundancy possibly being responsible for the more robust formation of anterior somites (see Oates and Ho, 2002; Sieger et al., 2003) is a matter of ongoing debate. Finally, also the involvement of additional signaling pathways is unclear. For example, the factors that induce the Tbx24 'wavefront' at proper locations remain unknown. The identification of additional factors and the detailed analysis of their interactions will therefore help to understand the complex networks leading to oscillating gene expression that consequently results in the repeated formation of somites.

To uncover novel components involved in segmentation, we carried out a large-scale mutagenesis screen in Medaka and identified mutants that show defects in somite formation. Several of these mutant share similar features with described zebrafish mutants, however, the majority of these mutants represent phenotypes unrecorded yet in zebrafish. These Medaka mutants provide clues to identifying new components as well as understanding conserved and divergent mechanisms underlying segmentation and somite formation.

2. Results

2.1. Medaka mutant embryos with defects in somite formation

In the large-scale mutagenesis screen in Medaka (Furutani-Seiki et al., this issue), we identified 12 mutations in nine genes affecting formation of somites. The mutants exhibit phenotypes characterized by the complete or partial absence of somites or somite boundaries (Fig. 1B–D,F; Table 1). Other mutations cause fused somites or somites with irregular sizes and shapes (Fig. 1G–K). All these are zygotic recessive embryonic lethal mutations while all the zebrafish mutations affecting somitogenesis, except *mindbomb* (*mib*; Itoh et al., 2003) and a *her1/her7* deficiency mutant (Henry et al., 2002), are viable. Therefore, mutant embryos refer to homozygotes of the mutation in the following description. Mutant embryos die shortly before hatching, except *schnelles ende* (*sne*) that survives several days after hatching. Unlike zebrafish mutants, some of the Medaka somitogenesis mutants also show other morphological defects particularly in head formation. These include

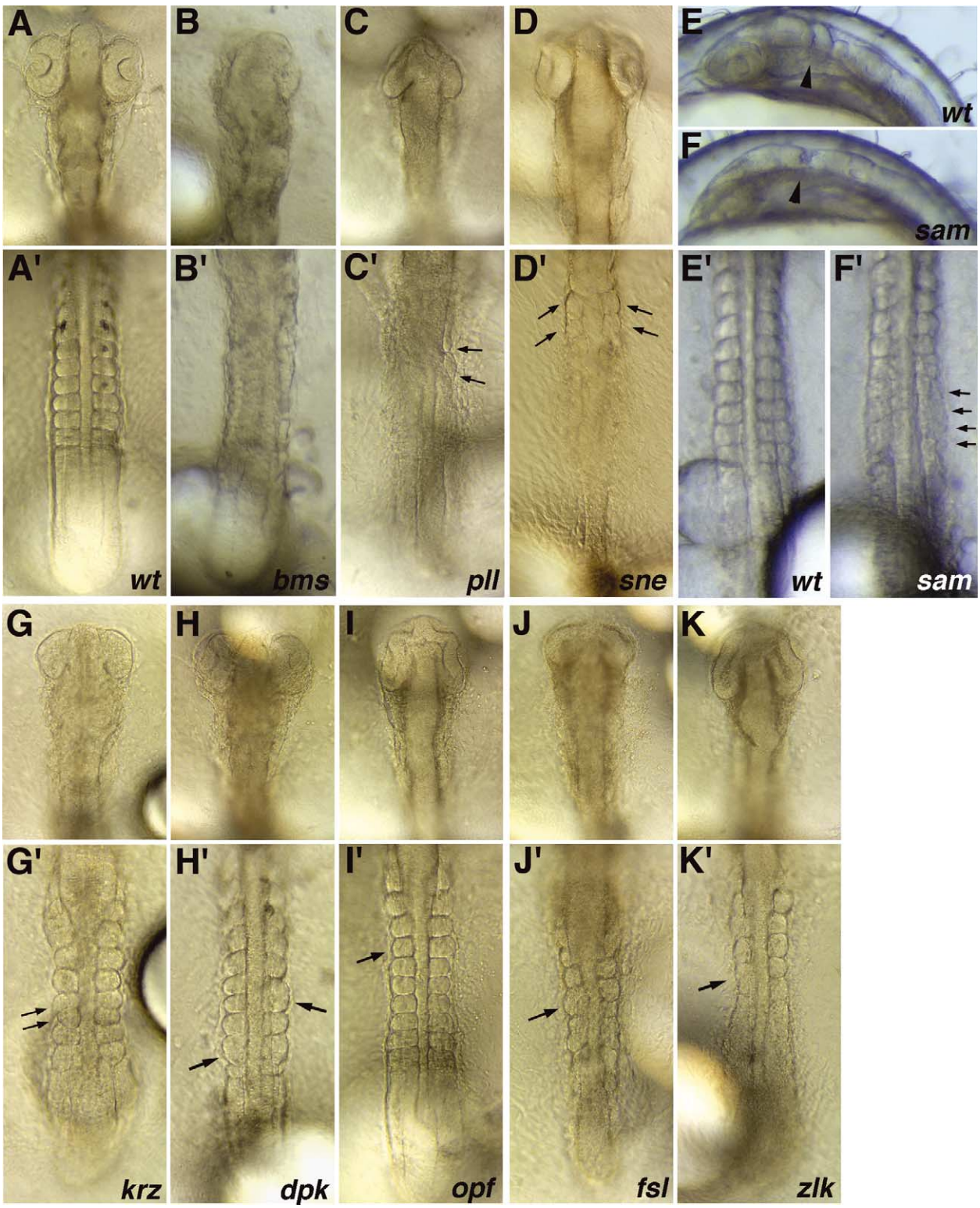

Fig. 1. Images of live Medaka embryos showing defects in somite formation. Dorsal views of head (A–K) and trunk (A′–K′) regions of wild-type (A,E) and different mutant (B–D, F–K) embryos at the 10–12 somite stage. Mutants either show a complete or partial lack of somite boundary formation (B–D,F) or exhibit irregular somite sizes and shapes (G–K). In some mutants, a degeneration or retardation of head development is evident (B,C,G–K) or the mid-hindbrain boundary does not form correctly (F).

Table 1
Classification of Medaka somitogenesis mutants based on morphology and expression at the 12 somite stage

Mutant	Alleles	Somitic phenotypes	Head phenotypes
Group 1: mutations affecting tailbud formation and PSM prepatterning			
bremser (*bms*)	*j20-22A*	No somites formed, only partial boundaries; *myf5* absent, *mesp* and *her7* reduced and irregular, absent *her7* oscillations	Arrested eye and forebrain morphogenesis
planlos (pll)	*j37-23A*	Partial formation of only 1–2 anterior somites; *myf5* absent, *mesp* strongly reduced, absent *her7* oscillations, *mesogenin* strongly reduced	Arrested eye and forebrain morphogenesis
schnelles ende (*sne*)	*j37-4A*, *j37-3B*, *j7-20B*, *j37-14A*	Only the first two somite pairs form, tailbud reduced; *myf5* only present in formed somites, *her7* strongly reduced, absent *her7* oscillations, *mesp* absent, *mesogenin* strongly reduced	Normal
samidare (*sam*)	*j20-26A*	No segmentation of posterior trunk, anterior six pairs of somites form normally; *myf5* reduced in posterior trunk, *mesp* reduced, *her7* discontinuous ('salt and pepper'), absent *her7* oscillations	Arrested eye and forebrain morphogenesis
doppelkorn (*dpk*)	*j14-17B*	Individually fused somites, irregular somite size; *myf5* and *mesp* irregular, *myf5* expanded in fused somites, *her7* expanded	Arrested eye and forebrain morphogenesis
Group 2: mutations affecting A-P-polarity and epithelialization			
kurzer (*krz*)	*j33-15C*	Variable somite shapes and sizes; *myf5* irregular and without stripe pattern, *lfng* reduced to small patches at lateral somite edges, *mesp* normal, regular *her7* oscillations	Arrested eye and forebrain morphogenesis
orgelpfeifen (*opf*)	*j6-24A*	Mild morphological phenotype with slightly irregular somite shapes and variable mediolateral extension; *myf5* nearly completely absent, *lfng* expanded into posterior somite domains, *pax3* reduced, *mesp* and *her7* normal, regular *her7* oscillations	Arrested eye and forebrain morphogenesis
fussel (*fsl*)	*j80-16A*	Individually fused somites, variable somite sizes; *myf5* expanded into anterior somite domains, *lfng* absent or strongly reduced, *mesp* normal, *her7* slightly reduced ('salt and pepper'), but regular *her7* oscillations	Necrotic
zahnluecke (*zlk*)	*j54-7B*	Irregular sizes and shapes of anterior somites, posterior somites partially missing; *myf5* reduced in posterior trunk, *mesp* and *her7* normal, regular *her7* oscillations	Arrested eye and forebrain morphogenesis

necrosis and retarded development of head structures (Fig. 1J), arrest of eye and forebrain morphogenesis (Fig. 1B,C, G–I,K) and defects in the formation of the mid-hindbrain boundary (Fig. 1F).

Mutant embryos of four genes, *bremser* (*bms*), *planlos* (*pll*), *schnelles ende* (*sne*) and *samidare* (*sam*), do not form the full complement of epithelialized somites. The *bms* mutant embryos exhibit the strongest phenotypes without distinct somite boundaries (Fig. 1B′). Somitic phenotypes in the *bms* mutant accompany defects in head formation (Fig. 1B). The mutant embryos of the remaining three genes fail to form somites posterior to the first pairs, a feature common to the zebrafish somite mutants in which Delta/Notch signaling is affected. However, the number of formed somites varies among these three mutants. In *pll* mutant embryos, only one or two incomplete somites are formed at the anterior-most edge of the paraxial mesoderm that are only partially epithelialized (Fig. 1C′). In this mutant, head formation is also affected (Fig. 1C). *sne* mutant embryos form two complete pairs of fully epithelialized somites of normal size and shape but completely lack all the remaining somites (Fig. 1D′). No apparent defects were observed in the head (Fig. 1D). *sam* mutant embryos show a phenotype similar to the *after eight* (*aei*) and *deadly seven* (*des*) zebrafish mutants, in which *deltaD* and *notch1a* are mutated, respectively (Holley et al., 2000, 2002). In both, *aei/des* and *sam* mutant embryos the first five to eight pairs of somites form normally, but somite boundaries are not formed in more posterior somites and the paraxial mesoderm remains unsegmented. Unlike *aei*, *des* and all other known zebrafish somite mutants, *sam* mutant embryos also do not form a distinct mid-hindbrain boundary (Fig. 1F).

Until the 10–12 somite stage, the mutants *kurzer* (*krz*), *doppelkorn* (*dpk*), and *orgelpfeifen* (*opf*) apparently form the correct number of somites. However, single somites are either fused or show irregular size and shape. In *krz*, the A-P length of the body axis is slightly shortened. Instead of an elongated shape, the somites have a round morphology, show variable size and are irregularly arranged along the notochord (Fig. 1G′). Also head formation is slightly delayed in this mutant (Fig. 1G). In *dpk*, single somites are fused at variable positions on either side of the notochord (Fig. 1H′). In the *opf* mutant, somite boundaries form normally, but somite sizes vary on either side of the embryo and show size differences along the medio-lateral

axis (arrow in Fig. 1I′). Compared to the wild-type situation (Fig. 1A′), this results in an irregular appearance of somites, when left and right embryo sides are compared.

Fused somites are also observed in embryos mutant for *fussel* (*fsl*) and *zahnluecke* (*zlk*) (Fig. 1J′,K′). In addition, these mutants also fail to form posterior somites, such that irregular somites are only present in the anterior trunk region. Both mutants also show severe head defects, characterized by a failure of eye morphogenesis (Fig. 1J,K).

During later stages of development, several mutants exhibit significantly shortened body axes and severe head defects (Fig. 2A–G). At this stage, most mutants also exhibit disorganized tailbuds (Fig. 2B′–G′) when compared to wild-type (Fig. 2A′). Somite boundaries are apparently

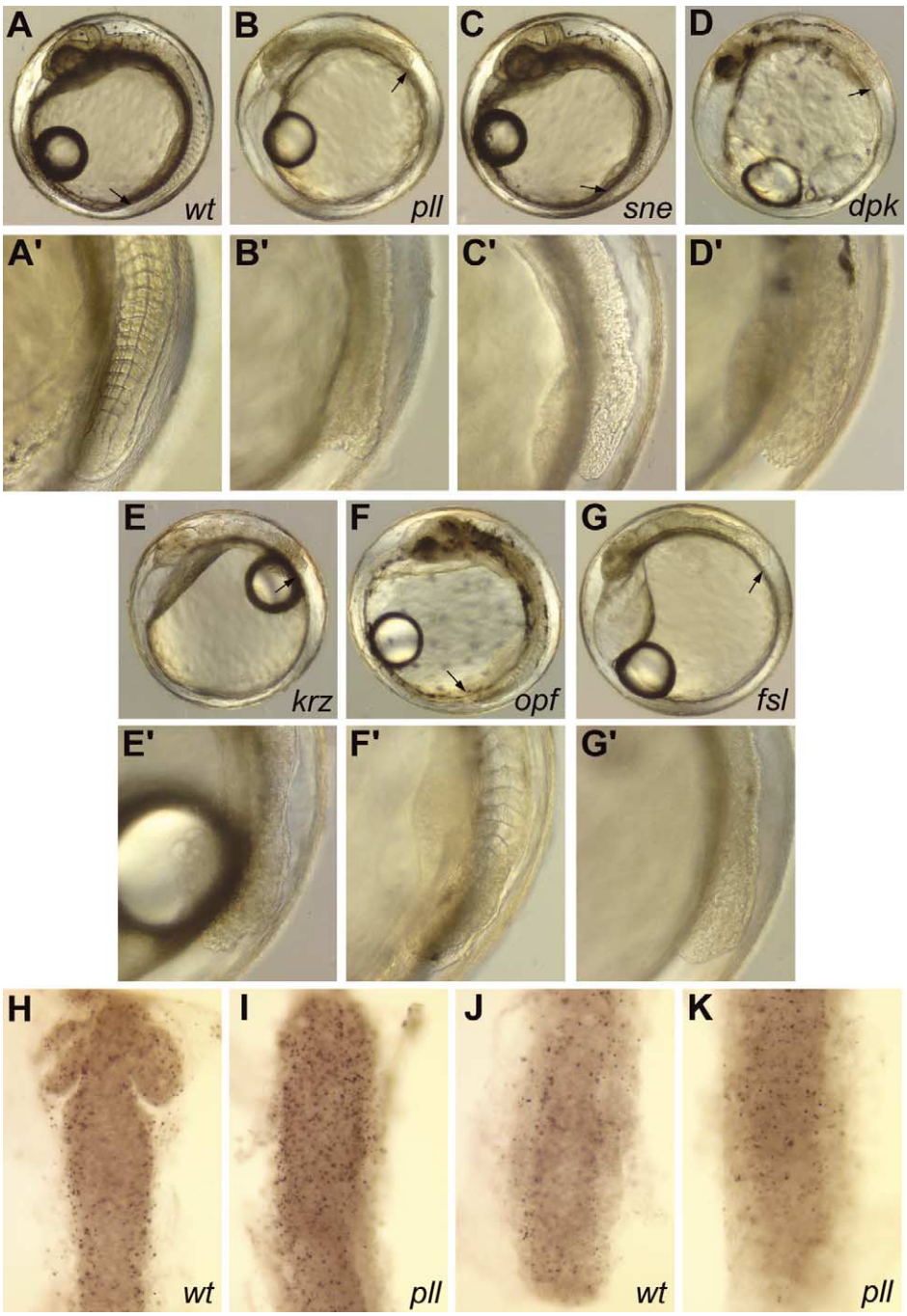

Fig. 2. Late phenotypes of medaka somitogenesis mutants. Lateral views of whole embryos (A–G) and tailbuds (A′–G′) at the 24–28 somite stage. Compared to a wild-type embryo (A,A′) most mutants exhibit shortened body axis and absence of trunk segmentation (except *opf*; F, F′) and severe head defects (except *sne*; C). The position of the tailbud is indicated by arrows in A–G. (H–K). Detection of apoptotic cells in wild-type (H,J) and *pll* mutant embryos (I,K) at the 5 somite stage. Note increase in apoptotic cell number in the head region of *pll* mutants (I) compared to wild-type (H), while apoptosis is not significantly altered in the trunk region of *pll* (K).

absent, with the exception of *opf* (Fig. 2F,F′) where trunk segmentation continues into late embryonic stages. Except *sne*, all other mutants show arrested head development that is likely due to increased apoptosis, as has been demonstrated for the *pll* mutant (Fig. 2I). Interestingly, however, apoptosis was not significantly increased in the *pll* trunk region (Fig. 2K) when compared to the wild-type situation (Fig. 2J). Taken together, Medaka somitogenesis mutants develop severe defects in addition to segmentation failure that unlike in zebrafish, but similar to the situation in mouse somite mutants result in early embryonic lethality.

2.2. Medaka somitogenesis mutants with defects in PSM prepatterning

For a more detailed characterization of somite phenotypes in these mutants, RNA in situ hybridization was performed using the Medaka orthologs of known somitogenesis markers as probes. As markers for the analysis of somite A-P polarity and patterning, Medaka *myf5* and *lunatic fringe* (*lfng*) were used. *myf5* is expressed in the caudal domain of individual somites, in the adaxial mesoderm and in the anterior PSM generating a striping pattern (Fig. 3A′; for details see Elmasri et al., 2004). On the other hand, *lfng* expression is restricted to the rostral somite domains (Fig. 4A″; Elmasri et al., 2004). Prepatterning of the PSM was examined by the expression of *mesp* and *her7*. *mesp* is expressed in the anterior-most PSM in one or two stripes, depending on the phase of somite formation (Fig. 3A′,A″) (Sawada et al., 2000; Elmasri et al., 2004). *her7* shows a highly dynamic expression in the PSM with one stripe of expression detaching from the posterior PSM and migrating rostrally (Fig. 3A″; Elmasri et al., 2004). Finally, *eng2* (Ristoratore et al., 1999) was used to detect defects in the formation of the mid-hindbrain boundary region.

Based on the expression of these molecular markers, we classified the somitogenesis mutants in 9 genes described above into two groups (Table 1). In group 1, all mutants show severe alterations of the dynamic pattern of *her7* expression in the PSM indicative for deficient prepattering in this region (Fig. 3). In contrast, in group 2 mutants somites are malformed and the expression patterns of *myf5* and *lfng* are altered, while these mutants exhibit apparently normal expression of *her7* and *mesp* in the PSM (Fig. 4).

In group 1, *bms* mutant embryos do not form any morphologically distinct somite boundaries (Fig. 1B′). *her7* expression in the PSM is reduced and lacks its characteristic dynamic oscillations (Fig. 3B″). *mesp* expression is present, but its expression domain appears irregular and not confined to one or two somitomeres (Fig. 3B′). *myf5* expression is completely absent from the trunk region except some transcripts that are found next to the PSM region (arrows in Fig. 3B′). The lack of localized *myf5* expression and somite boundaries suggests the absence of any somitic differentiation.

Like the *bms* mutant, *pll* mutant embryos also lack visible somite boundaries, except for one or two irregularly formed somites in the most anterior trunk region (arrows in Fig. 1C′). While in *pll* mutant embryos the level of *her7* expression in the posterior PSM appears unaltered, again no oscillations of *her7* expression were evident (Fig. 3C). Furthermore, *mesp* expression is significantly reduced (see arrows in Fig. 3C′). No *myf5* transcripts are detectable, neither in the posterior trunk, nor in the 1 or 2 somites formed anteriorly, suggesting that these somitic mesodermal remnants do not possess polarity or myogenic identity.

sne mutant embryos show, in contrast, expression of *myf5* in the two pairs of somites visible in the anterior trunk (Figs. 1D′,3D′). However, *myf5* is not expressed in more posterior regions, and also *mesp* is completely absent (Fig. 3D′,D″). Despite the lack of most of the posterior trunk, weak expression of *her7* is detected in the PSM (Fig. 3D″). This *her7* expression is located in the most posterior region of the PSM. In a few cases, expression was also found in more anterior regions and on one side of the embryo (arrow in Fig. 3D″). This unilateral expression appeared randomly positioned and possibly indicates remaining *her7* oscillation.

To analyze whether the effects seen in *pll* and *sne* are due to deficient PSM prepatterning or to earlier defects during specification of the tailbud mesoderm, we analyzed the expression of *mesogenin* in *pll* and *sne*. *mesogenin* is uniformly expressed in the tailbud of wild-type zebrafish (*mespo*; Yoo et al., 2003) and Medaka (Fig. 3G). Despite remaining *her7* expression in the tailbud of especially *pll* (Fig. 3C″), hardly any expression of *mesogenin* could be detected (Fig. 3H,I). This suggests that the defects seen in *pll* and *sne* result from early deficiencies in tailbud formation. It also indicates that the somites identified in the anterior-most trunk region of *pll* and *sne* mutants apparently form independently from a correctly specified tailbud.

The two remaining members in this group of PSM deficient mutants, *sam* and *dpk*, form somite boundaries and show *myf5* expression, however, in irregular patterns. In *sam* mutant embryos, the first six pairs of somites form normally (Fig. 1F′) and show regular *myf5* expression (Fig. 3E′). The more posterior somites, however, do not form correctly and show significantly reduced levels of *myf5* expression in the region that lacks visible somite boundaries (arrows in Fig. 3E′). On the other hand, *myf5* expression in the adaxial mesoderm and anterior PSM (Fig. 3E′), as well as *mesp* expression (Fig. 3E″) appears normal. In *sam* mutant embryos, *her7* shows an uneven distribution across the PSM. Cells located in a horseshoe shaped area in the anterior PSM exhibit high levels of expression, while expression is strongly reduced in neighboring cells. This pattern is similar to the ‘salt-and-pepper’ pattern described for *her1* and *her7* in *delta/notch* deficient zebrafish mutants (Holley et al., 2002; Oates and Ho, 2002). The *sam* mutant embryos show a failure in formation of the mid-hindbrain

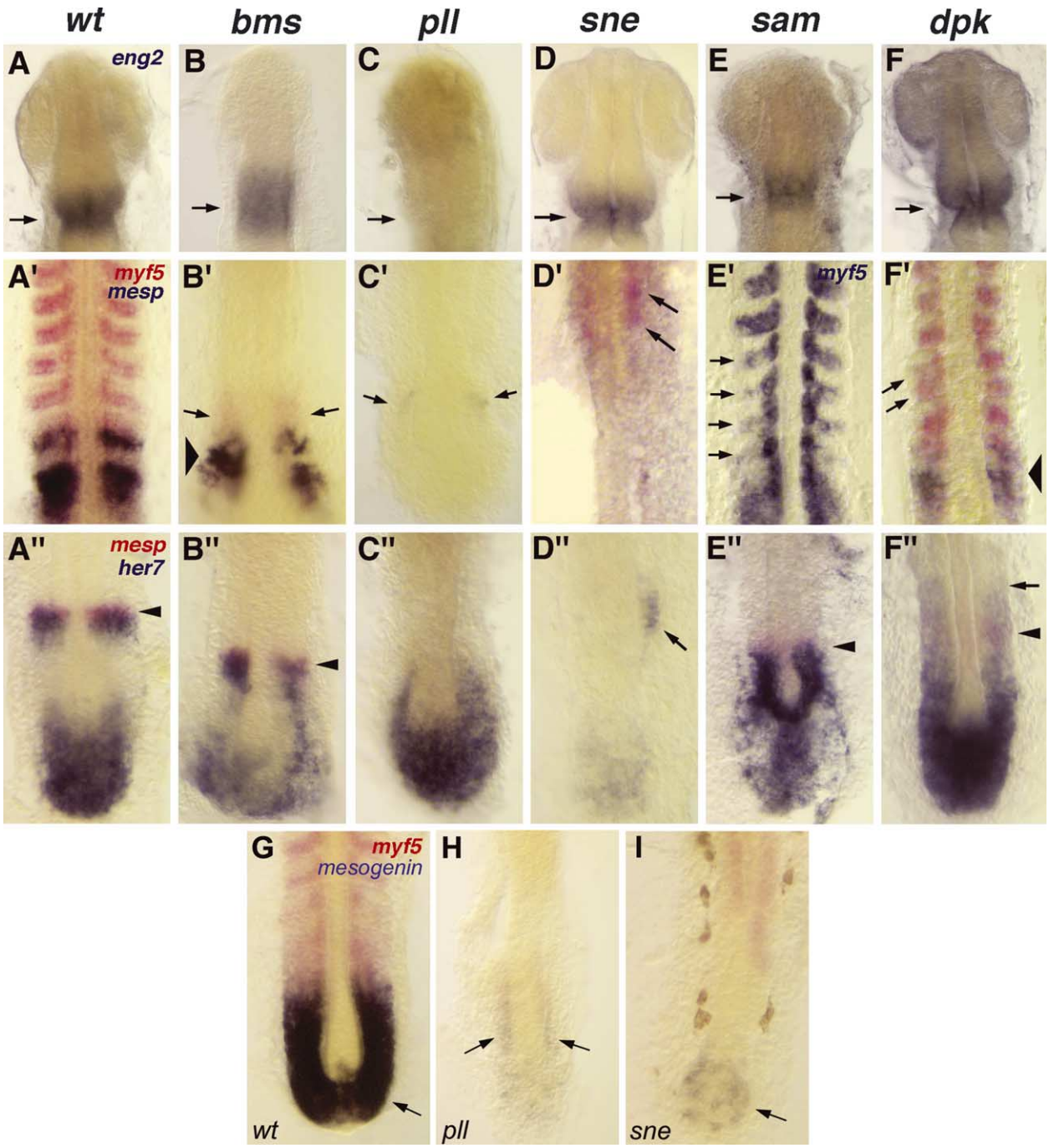

Fig. 3. Medaka somite mutants with deficient gene expression in the presomitic mesoderm (PSM). Analysis of *eng2* gene expression at the mid-hindbrain boundary (A–F), *myf5* (in red) and *mesp* expression (in blue; except E′ that shows *myf5* in blue, but no *mesp*) in the somitic trunk (A′–F′) and *her7* and *mesp* in the PSM (A″–F″). All images are dorsal views of embryos at the 10–12 somite stage with anterior to the top, the mutant names are given on top of each column. All mutant lines (B″–F″) exhibit non-dynamic and deficient *her7* expression. This includes overall reduced expression levels (B″,D″,E″), 'salt-and-pepper' expression patterns (E″) or failure of *her7* down-regulation in the anterior PSM (F″; arrow indicates anterior extension of *her7* domain; *mesp* expression in the anterior-most PSM is marked by arrowheads). *myf5* expression in caudal somite halves is either partially (B′,D′,E′; remaining *myf5* marked by arrows) or completely lost (C′; remaining *mesp* marked by arrows) or indicates fusion of somites and irregular A–P polarity (arrows in F′; arrowheads mark *mesp* expression). Except *sne* (D), all mutants show a smaller head with partially reduced *eng2* expression (arrows in B–F). (G–I). Analysis of mesogenin expression in the tailbuds of wild-type (G), *pll* (H) and *sne* (I) mutant embryos.

boundary, and expression of *eng2* is slightly reduced (Figs. 1F,3E). This is very similar to the situation in the zebrafish mid-hindbrain boundary mutants *acerebellar* (*ace/fgf8*; Reifers et al., 1998) and *no-isthmus* (*noi/pax2b*; Lun and Brand, 1998), where *eng2* is also reduced at the 12-somite stage.

In the *dpk* mutant embryos, individual neighboring somites are fused at random positions along

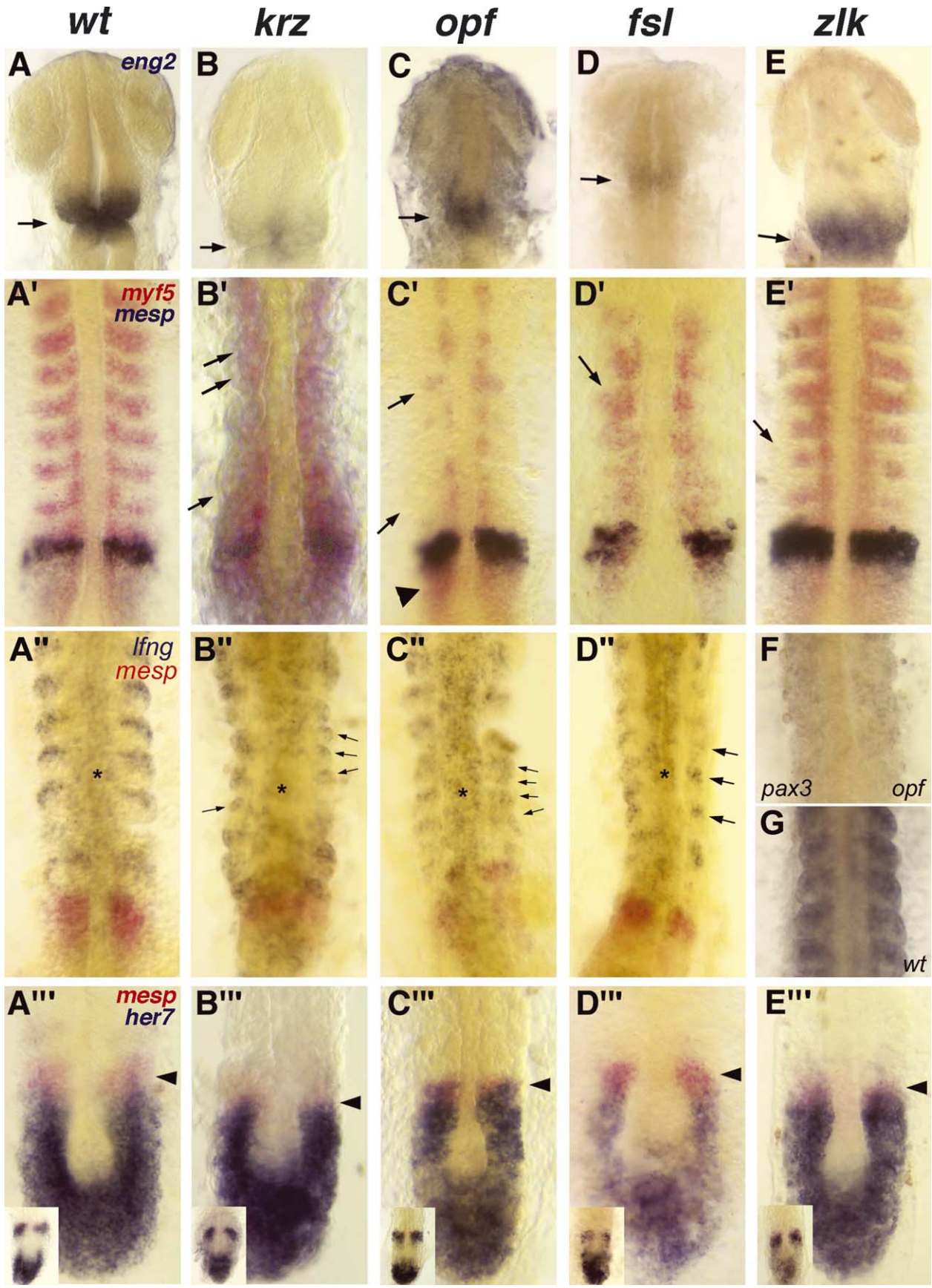
wt
krz
opf
fsl
zlk
A
eng2
B
C
D
E
A'
myf5
mesp
B'
C'
D'
E'
A''
lfng
mesp
B''
C''
D''
F
pax3
opf
G
wt
A'''
mesp
her7
B'''
C'''
D'''
E'''

the anterior-posterior axis of the trunk. This is reflected by the fusion of *myf5* domains in the paraxial mesoderm (Fig. 3F′), suggesting that A-P polarity might be affected. Intriguingly, *her7* is not downregulated in the anterior PSM. Instead, the *her7* expression domain extends far into the region of the formed somites (arrow in Fig. 3F″) and even passes the domain of *mesp* expressing cells (arrowhead in Fig. 3F″). This is never observed in wild-type control embryos (Fig. 3A″). It suggests that the *dpk* mutation affects the stabilization of *her7* expression in the anterior PSM and interferes with down-regulation of *her7* expression in more rostral regions.

2.3. Medaka somitogenesis mutants with aberrant somite polarity but normal PSM expression

In the group 2 mutant embryos, *her7* and *mesp* expression patterns are apparently normal, but somite boundaries are irregular and *myf5* expression is affected.

krz mutant embryos show irregular somite sizes and slightly delayed head development as seen by reduced *eng2* expression in the mid-hindbrain boundary region (Fig. 4B). In the irregular somites, expression of *myf5* is not localized to the caudal half of the somite, but instead is expressed in a discontinuous and non-segmental pattern throughout the somites (Fig. 4B′). This suggests a failure in establishing the A-P polarity in these somites, probably resulting in a subsequent failure of correct somite differentiation. Consistent with this, also *lfng* expression in the rostral domains of individual somites is affected and shows reduced expression that is restricted to the tips of single somites (arrows in Fig. 4B″). In the *krz* mutant embryos, however, PSM prepatterning is unaffected. Both, *her7* and *mesp* are expressed in the PSM with their normal and dynamic patterns (Fig. 4B‴).

Somite formation in the *opf* mutant is only mildly affected at the morphological level, with some minor asymmetries in somite sizes, when bilateral trunk segments are compared (arrow in Fig. 1I′). The expression of *myf5* is strongly reduced, while *mesp* (Fig. 4C‴) and *her7* (Fig. 4C‴) are expressed at apparently normal levels. *myf5* expression is detected in the anterior PSM (arrowhead in Fig. 4C′) and at low levels also in the adaxial mesoderm, but nearly no *myf5* transcripts are present in the paraxial mesoderm (arrows in Fig. 4C′). On the other hand, expression of the anterior marker *lfng* appears expanded along the entire A-P axis of individual somites (arrows in Fig. 4C″). This suggests that somites might be anteriorized, but additional markers are needed to confirm this. Thus, while PSM prepatterning and somite boundary formation is normal, A-P polarity appears affected in the *opf* mutant. Consistent with the idea that the lack of *myf5* could possibly reflect defects in the myogenic lineage, also *pax3* transcripts are reduced and aberrantly distributed across *opf* somites (Fig. 4F). In mouse, *pax3* is a dermomyotome marker that is expressed broadly within the early PSM/somite, and becomes restricted to hypaxial precursors later (Tremblay et al., 1998).

In *fsl* mutant embryos, in contrast, *myf5* expression is expanded antero-posteriorly in the paraxial mesoderm (Fig. 4D′). Morphologically, this mutant shows enlarged and partially fused somites (Fig. 1J′). The majority of cells in each somite expresses *myf5* suggesting that also in this mutant A-P polarity is impaired and a posteriorization could have occurred in the early somitomeres. This is also suggested by the expression of *lfng* that is either absent or shows strongly reduced levels in *fsl* (Fig. 4D″) when compared to wild-type embryos (Fig. 4A″). In the PSM, *mesp* expression however appears not affected and *her7* oscillation occurs normally (Fig. 4D‴). Expression of *her7* is slightly reduced and exhibits a ‘salt-and-pepper’ pattern (Fig. 4D‴), but this is less pronounced compared to the *sam* mutant (Fig. 3E″).

zlk mutant embryos show a phenotype similar to that of *sam* mutants. In both mutant embryos, the first pairs of somites form more or less normally, but formation of more posterior somites is impaired. However, unlike in *sam*, the anterior somites show irregular shape and size in *zlk* mutant embryos. Moreover, there are significant differences in the expression of markers. In contrast to *sam*, *zlk* mutant embryos show normal expression of *mesp* and *her7* (Fig. 4E‴). In addition, only a weak reduction of *myf5* is evident in the posterior somites (arrow in Fig. 4E′). These results suggest deficiencies in late phases of somite formation, e.g. steps of somite differentiation that are independent from processes in the PSM.

Fig. 4. Somitogenesis mutants with irregular somite differentiation, but regular PSM expression. All mutant embryos shown (B‴–E‴; control in A‴) exhibit regular and dynamic expression of *her7* and *mesp* (arrowheads) in the PSM, but deficient *myf5* expression in formed somites (arrows in B′–E′). This includes irregular *myf5* expression throughout somitic region (B′), missing (C′) or reduced *myf5* (E′) in caudal somite halves, and anterior expansion of *myf5* in fused somites (D′; labeled by arrows). The arrowhead in C′ marks remaining *myf5* expression in the anterior PSM. Also *lfng* expression in the rostral domains of individual somites is affected in *krz*, *opf* and *fsl* embryos (B″–D″). In *opf*, *pax3* expression is reduced and uniformly distributed across the somites (F) when compared to the wild-type situation (G). Other than in wild-type controls (A), all mutant embryos (B–E) also exhibit delayed head formation (*eng2* expression marked by arrows). Small insets in A‴–E‴ show *her7* and *mesp* expression at different, i.e. advanced phases of the somitogenesis cycle and indicate normal expression of *her7* in the PSM. All images are dorsal views of embryos at the 10–12 somite stage, anterior is to the top. Asterisks in A″–D″ mark *lfng* expression in the neural tube.

3. Discussion

3.1. Two distinct groups of Medaka somitogenesis mutants

In the Medaka, every cycle of somite formation takes approximately 1 h at 26 °C. Under wild-type conditions, formation of the full complement of 35 somite pairs is completed after 3.5 days post fertilization (Iwamatsu, 1994). Here, we have described nine different mutations that result in various deficiencies during somitogenesis. Although several mutants look very similar at the morphological level, they show significant differences in the expression of established markers for somite formation and differentiation. This allowed us to group all mutants into two groups. Group 1 mutants show defects in tailbud formation and PSM prepatterning and consequently impaired somite development. Group 2 mutants do not have apparent alterations in PSM expression of *her7* and *mesp*, indicating that PSM prepatterning is not affected. They nevertheless fail to form regularly shaped and sized somites and show deficient A-P polarity suggesting defects in later phases of somite formation.

Several group 1 mutants lack posterior somites and only form varying numbers of epithelialized somites in the anterior trunk. They show different aspects of *her7* expression, ranging from nearly complete absence to rather normal expression levels. However, all group 1 mutants share the lack of dynamic *her7* oscillations indicating deficiencies in integral components of the segmentation clock. Of particular interest is the *dpk* mutant that shows partially fused somites and irregular somite size. In *dpk*, *her7* expression extends into the already formed somites, rather than being stabilized in the anterior PSM as in wild-type zebrafish (Oates and Ho, 2002) and Medaka (Elmasri et al., 2004). Periodic stabilization of *her1* and *her7* in the anterior-most PSM is crucial for correct formation of the next somite boundaries. This stabilization is regulated by a molecular 'wavefront' that is generated by the activity of *tbx24* (Nikaido et al., 2002) and possibly other, so far unknown factors. Zebrafish *fss* mutants that are deficient for *tbx24* fail to stabilize oscillating Notch activity in the anterior PSM, lack the anterior-most stripe of *her1* expression and show no *mespb* expression (Nikaido et al., 2002). Consequently, *fss* mutants do not form any somite boundaries along the entire body axis (van Eeden et al., 1996). In contrast to this, the Medaka *dpk* mutant shows an expansion of the *her7* expression domain, with apparently normal *mesp* expression levels in the anterior PSM. This indicates an excess of Notch target stabilization rather than a destabilization as seen in zebrafish *fss*. Therefore, this suggests that the wavefront is up-regulated in *dpk* and opens the possibility that this mutant carries a mutation in a gene encoding an upstream component of the wavefront. It is also possible that FGF signaling is affected in this mutant, as this pathway is known to antagonize *tbx24* (Sawada et al., 2001). Alternatively, *dpk* mutants could also have a defect in the negative feedback loop that downregulates *her7* similar to the situation observed in *her1*/*her7* morpholino injected embryos (Holley et al., 2002). So far, however, no zebrafish mutant has been described that shows extended expression of a Notch target gene in the PSM.

3.2. Medaka mutants with somite polarity defects

So far, all five known zebrafish mutants that show defects in somite boundary formation (*aei*, *des*, *bea*, *wit* and *fss*; van Eeden et al., 1996) also show perturbations in the expression of oscillating genes in the PSM. Consequently, A-P segment polarity is abolished and somite boundaries fail to form. None of the zebrafish somitogenesis mutants shows normal PSM prepatterning. In contrast to this, we have identified the Medaka mutants *krz*, *opf* and *fsl* that show apparently normal oscillating expression of *her7*, however, exhibit abnormal A-P patterning within individual somites. These mutants therefore represent good candidates for deficiencies that affect the later phases of somite formation and differentiation. This could include processes for the determination of A-P polarity that are independent from a *her1-her7* controlled oscillation circuit. Alternatively, these mutations possibly affect components that translate oscillator output information into the A-P identity of cells in the rostral PSM. So far, these processes are poorly understood at the molecular level and no corresponding mutants have been described in zebrafish.

In the Medaka, we have identified mutants that either show an expansion (*krz*; *fsl*) or a reduction of *myf5* expression (*opf*; *zlk*), but with apparently normal oscillator activity. While an expansion of *myf5* with a coincident reduction of *lfng* indicates posteriorization of somitomeres, *myf5* reduction could be interpreted as a possible anteriorization. Alternatively, myogenic determination could be suppressed in these mutants. Our observation that *lfng* is expanded in *opf* mutants is in agreement with the anteriorization hypothesis. However, clearly more markers need to be analyzed in the future to clarify this point. Nevertheless, it is tempting to speculate that the molecular identification of these mutations will reveal factors that establish the A-P polarity of somites in an oscillator-independent manner.

3.3. A comparison of Medaka and zebrafish somitic phenotypes: mutations affecting posterior somite formation

Several group 1 phenotypes clearly resemble those of described zebrafish somitogenesis mutants. They only form anterior somites, a hallmark characteristic for the zebrafish Delta/Notch mutants *after eight* (*deltaD*; Holley et al., 2000), *beamter* (*bea*; van Eeden et al., 1996), and *deadly seven* (*notch1a*; Holley et al., 2002). Importantly, however, we also identified mutants with phenotypes that have not been described in zebrafish so far. These include several mutants with locally fused somites, differences in somite

size, and an irregular arrangement of somite boundaries. Thus, these Medaka mutants partially resemble mouse segmentation mutants, where somite fusions have been described e.g. in knock-out mice deficient for *Hes7* (Bessho et al., 2001).

In group 1, *sam* mutant embryos show a particularly interesting phenotype. The first seven pairs of somites form normally, but boundary formation in more posterior somites fails. This is similar to the defects seen in the zebrafish *aei/deltaD* and *des/notch1* mutants. In the PSM of *des*, *her1* shows a typical 'salt-and-pepper' expression pattern (Holley et al., 2002), which was explained as a consequence of the breakdown of oscillation and synchronization of Notch signaling between neighboring cells (Jiang et al., 2000). This situation could be similar in the *sam* mutant, where a 'salt-and-pepper' expression of *her7* was observed. However, in contrast to all known zebrafish somitogenesis mutants, *sam* also shows a defect in the formation of the mid-hindbrain boundary. Defects in this structure, on the other hand, were observed in the zebrafish *fgf8* mutant *acerebellar* (*ace*; Reifers et al., 1998). Therefore, it is tempting to speculate that *sam* is affected in the FGF signaling pathway. This possibility is of particular interest, as it was shown that FGF signaling is important for somite formation in chicken and zebrafish (Dubrulle et al., 2001; Sawada et al., 2001). However, no somitogenesis mutants with defects in FGF signaling have so far been identified in the zebrafish screens. The reason that zebrafish *ace* mutants show only a very mild somitic phenotype was explained by functional redundancy by other FGF encoding genes (e.g. *fgf24*) that compensate deficient FGF8 signaling in the trunk region (see Draper et al., 2003).

3.4. Diversification of genetic redundancy—towards the molecular identification of the segmentation clock in fish

The analysis of mutants from the large-scale mutagenesis screens in zebrafish has significantly contributed to our understanding of somitogenesis. Mutant analysis and subsequent gene knock-down studies resulted in a model for the molecular oscillator (reviewed in Holley and Takeda, 2002). This model puts *her1* and *her7* as central components of the somitogenesis clock responsible for the generation of oscillatory circuits. *her1* and *her7* encode transcriptional repressors that establish autoregulatory loops. These loops involve other components of the Notch pathway and result in oscillating gene transcription of *her1*, *her7* and *deltaC* (Holley et al., 2002; Oates and Ho, 2002). In the posterior PSM, this periodic transcription is propagated across neighboring cells (Jiang et al., 2000). Consequently, this causes periodic waves of gene transcription that travel through the PSM. Although this represents an attractive model to explain oscillating gene transcription, it should be noted that the view of autoregulatory repression of *her1* and *her7* as central part of this model recently has been challenged (Gajewski et al., 2003). There, the authors postulate an activating rather than repressing activity of Her1 and Her7.

In addition, the small number of identified zebrafish mutants is surprising given the complexity of this process. With one exception (*fused somites*; Nikaido et al., 2002), all identified mutants are affected in the Delta/Notch pathway. However, recent studies have clearly demonstrated that additional signaling pathways are critical regulators of somite formation (reviewed in Pourquie, 2003). No zebrafish somite mutants have been identified e.g. in the FGF or Wnt signaling pathways, although the importance of these has been shown in several vertebrate models (Sawada et al., 2001; Aulehla et al., 2003). Furthermore, it is surprising that all known zebrafish Delta/Notch somite mutants, except *mib* and a *her1/her7* deficiency, are homozygous viable and fertile, whereas the corresponding mutant mice are embryonic lethal. In Medaka, all mutant lines described here are early lethal and show additional morphological defects, similar to the situation in mouse.

One possible explanation for the lack of FGF or Wnt somitogenesis mutants in zebrafish is functional redundancy as a consequence of gene duplication events. In fish, many developmentally important regulatory genes exist as duplicates that originated in the teleost lineage (Amores et al., 1998; Wittbrodt et al., 1998; Meyer and Schartl, 1999; McClintock et al., 2001). These duplicates often show partially overlapping functions, as has been shown e.g. for the Wnt and Hedgehog pathways in zebrafish (Lewis and Eisen, 2001; Lekven et al., 2003). Thus, it would require simultaneous mutation in both duplicated genes in order to result in a visible deficiency. Importantly, the number of duplicated genes in fish varies from species to species (see Naruse et al., 2000; Amores et al., 2004). Accordingly, significant differences have been reported when the genomes of zebrafish, Fugu and Medaka were compared (e.g. Amores et al., 1998, 2004; Naruse et al., 2000; Winkler et al., 2003a). These variations are explained by the differential behavior of duplicated copies after local or genome-wide duplications during evolution. In both cases, distinct levels of functional redundancy can be expected dependent on the species analyzed. Therefore, it is possible that random mutagenesis leads to distinct somite phenotypes in different fish species.

Taken together, we have characterized nine mutations affecting somite formation in Medaka. The observed defects cover all phases of somite formation, i.e. PSM prepatterning, A-P polarity and establishment of somite boundaries. While some aspects in these mutants are similar to those found in zebrafish mutants, we also found significant differences in somite mutants between zebrafish and Medaka. Hence, the molecular characterization of the mutated genes should lead to the identification of factors that so far have not been implicated in somitogenesis or possibly even to the isolation of novel components involved in this process.

4. Experimental procedures

4.1. Mutagenesis screen and maintenance of mutant fish strains

We carried out a mutagenesis screen as described elsewhere (Furutani-Seiki et al., this issue). Adult mutant carriers were maintained at a 14 h/10 h light cycle to induce spawning. Egg clutches were collected from the females every morning and transferred to dishes with embryo medium for further examination. Embryonic stages were determined according to Iwamatsu (1994).

4.2. Life images

For life images, embryos were incubated in 10 mg/ml proteinase K for 3 h at 29 °C to remove hair filaments from the outside of the chorion. Embryos were rinsed in embryo medium and then mounted in 3% methylcellulose in embryo medium. Pictures were taken on a Zeiss Axiophot microscope with a Sony HC2000 digital camera and assembled using the Adobe Photoshop v6.0 software package on a Macintosh computer.

4.3. RNA in situ hybridizations

One and two-color whole mount in situ hybridizations were done as described (Winkler et al., 2003b). For analysis of somite formation and patterning, the following probes were used: *Oryzias latipes her7*, *mesp*, *lfng* and *myf5*. The cloning and a detailed description of the expression patterns of these markers is described elsewhere (Elmasri et al., 2004), except for *pax3* (J. Renn and CW, unpublished) and *mesogenin* (H.E. and C.W., unpublished). For the analysis of mid-hindbrain boundary defects, the Medaka *eng2* probe was used (Ristoratore et al., 1999). For photography, stained embryos were removed from their yolk sac and flat-mounted in glycerol.

4.4. Detection of apoptosis

Embryos fixed in 4% paraformaldehyde/PBST and stored in 100% methanol were rehydrated in PBST/methanol. Apoptotic cells were visualized using the 'ApopTag Apoptosis Detection Kit' from Serologicals Corporation (Norcross, USA) according to the manufacturers recommendations. For detection, a peroxidase-coupled anti-digoxigenin antibody was used with diaminobenzidine as chromogenic substrate.

Acknowledgements

We thank Manfred Schartl for critical comments and constant support, Cordula Neuner for excellent technical assistance, Joerg Renn for providing the *pax3* riboprobe prior to publication and Marianne Schaedel for help with mutant stock keeping. This project was supported by the ERATO grant of Japan Science and Technology Agency (JST) to H.K. and the grant 50WB0152 of the DLR (Deutsches Zentrum für Luft-und Raumfahrt e.V.) to C.W.

References

Amores, A., Force, A., Yan, Y.L., Joly, L., Amemiya, C., Fritz, A., et al., 1998. Zebrafish *hox* clusters and vertebrate genome evolution. Science 282, 1711–1714.

Amores, A., Suzuki, T., Yan, Y.L., Pomeroy, J., Singer, A., Amemiya, C., et al., 2004. Developmental roles of pufferfish hox clusters and genome evolution in ray-fin fish. Genome Res. 14, 1–10.

Aulehla, A., Wehrle, C., Brand-Saberi, B., Kemler, R., Gossler, A., Kanzler, B., et al., 2003. Wnt3a plays a major role in the segmentation clock controlling somitogenesis. Dev. Cell 4, 395–406.

Bessho, Y., Sakata, R., Komatsu, S., Shiota, K., Yamada, S., Kageyama, R., 2001. Dynamic expression and essential functions of *Hes7* in somite segmentation. Genes Dev. 15, 2642–2647.

Draper, B.W., Stock, D.W., Kimmel, C.B., 2003. Zebrafish *fgf24* functions with *fgf8* to promote posterior mesodermal development. Development 130, 4639–4654.

Dubrulle, J., McGrew, M.J., Pourquie, O., 2001. FGF signaling controls somite boundary position and regulates segmentation clock control of spatiotemporal Hox gene activation. Cell 106, 219–232.

van Eeden, F.J.M., Granato, M., Schach, U., Brand, M., Furutani-Seiki, M., Haffter, P., et al., 1996. Mutations affecting somite formation and patterning in the zebrafish, Danio rerio. Development 123, 153–164.

Elmasri, H., Liedtke, D., Lücking, G., Volff, J.-N., Gessler, M., Winkler, C., 2004. *her7* and *hey1*, but not *lunatic fringe* show dynamic expression during somitogenesis in Medaka (*Oryzias latipes*). Gene Expression Pattern in press.

Gajewski, M., Sieger, D., Alt, B., Leve, C., Hans, S., Wolff, C., et al., 2003. Anterior and posterior waves of cyclic *her1* gene expression are differentially regulated in the presomitic mesoderm of zebrafish. Development 130, 4269–4278.

Henry, C.A., Urban, M.K., Dill, K.K., Merlie, J.P., Page, M.F., Kimmel, C.B., et al., 2002. Two linked hairy/enhancer of split-related zebrafish genes, *her1* and *her7*, function together to refine alternating somite boundaries. Development 129, 3693–3704.

Holley, S.A., Takeda, H., 2002. Catching a wave: the oscillator and wavefront that create the zebrafish somite. Semin. Cell Dev. Biol. 13, 481–488.

Holley, S.A., Geisler, R., Nüsslein-Volhard, C., 2000. Control of *her1* expression during zebrafish somitogenesis by a Delta-dependent oscillator and an independent wave-front activity. Genes Dev. 14, 1678–1690.

Holley, S.A., Julich, D., Rauch, G.J., Geisler, R., Nusslein-Volhard, C., 2002. Her1 and the notch pathway function within the oscillator mechanism that regulated zebrafish somitogenesis. Development 129, 1175–1183.

Itoh, M., Kim, C.H., Palardy, G., Oda, T., Jiang, Y.J., Maust, D., et al., 2003. Mind bomb is a ubiquitin ligase that is essential for efficient activation of Notch signaling by Delta. Dev. Cell 4, 67–82.

Jiang, Y.J., Aerne, B.L., Smithers, L., Haddon, C., Ish-Horowicz, D., Lewis, J., 2000. Notch signaling and the synchronization of the somite segmentation clock. Nature 408, 475–479.

Jouve, C., Palmeirim, I., Henrique, D., Beckers, J., Gossler, A., Ish-Horowicz, D., et al., 2000. Notch signalling is required for cyclic expression of the hairy-like gene HES1 in the presomitic mesoderm. Development 127, 1421–1429.

Iwamatsu, T., 1994. Stages of normal development in the Medaka *Oryzias latipes*. Zool. Sci. 11, 825–839.

Leimeister, C., Dale, K., Fischer, A., Klamt, B., Hrabe de Angelis, M., Radtke, F., et al., 2000. Oscillating expression of *c-hey2* in the presomitic mesoderm suggests that the segmentation clock may use combinatorial signaling through multiple interacting bHLH factors. Dev. Biol. 227, 91–103.

Lekven, A.C., Buckles, G.R., Kostakis, N., Moon, R.T., 2003. Wnt1 and wnt10b function redundantly at the zebrafish midbrain–hindbrain boundary. Dev. Biol. 254, 172–187.

Lewis, K.E., Eisen, J.S., 2001. Hedgehog signaling is required for primary motoneuron induction in zebrafish. Development 128, 3485–3495.

Lun, K., Brand, M., 1998. A series of no *isthmus* (*noi*) alleles of the zebrafish *pax2.1* gene reveals multiple signaling events in development of the midbrain–hindbrain boundary. Development 125, 3049–3062.

McClintock, J.M., Carlson, R., Mann, D.M., Prince, V.E., 2001. Consequences of Hox gene duplication in the vertebrates: an investigation of the zebrafish Hox paralogue group 1 genes. Development 128, 2471–2484.

Meyer, A., Schartl, M., 1999. Gene and genome duplications in vertebrates: the one-to-four (-to-eight in fish) rule and the evolution of novel gene functions. Curr. Opin. Cell Biol. 11, 699–704.

Naruse, K., Fukamachi, S., Mitani, H., Kondo, M., Matsuoka, T., Kondo, S., et al., 2000. A detailed linkage map of Medaka, *Oryzias latipes*. Comparative genomics and genome evolution. Genetics 154, 1773–1784.

Nikaido, M., Kawakami, A., Sawada, A., Furutani-Seiki, M., Takeda, H., Araki, K., 2002. Tbx24, encoding a T-box protein, is mutated in the zebrafish somite-segmentation mutant fused somites. Nature Genet. 31, 195–199.

Oates, A.C., Ho, R.K., 2002. *Hairy*/*E*(*spl*)-*related* (*Her*) genes are central components of the segmentation oscillator and display redundancy with the Delta-Notch signaling pathway in the formation of anterior segmental boundaries in the zebrafish. Development 129, 2929–2946.

Pourquie, O., 2001. Vertebrate somitogenesis. Annu. Rev. Cell Dev. Biol. 17, 311–350.

Pourquie, O., 2003. The segmentation clock: converting embryonic time into spatial pattern. Science 301, 328–330.

Reifers, F., Bohli, H., Walsh, E.C., Crossley, P.H., Stainier, D.Y., Brand, M., 1998. Fgf8 is mutated in zebrafish acerebellar (ace) mutants and is required for maintenance of midbrain–hindbrain boundary development and somitogenesis. Development 125, 2381–2395.

Ristoratore, F., Carl, M., Deschet, K., Richard-Parpaillon, L., Boujard, D., Wittbrodt, J., et al., 1999. The midbrain–hindbrain boundary genetic cascade is activated ectopically in the diencephalon in response to the widespread expression of one of its components, the Medaka gene Ol-eng2. Development 126, 3769–3779.

Saga, Y., Takeda, H., 2001. The making of the somite: molecular events in vertebrate segmentation. Nature Rev. Genet. 2, 835–845.

Sawada, A., Fritz, A., Jiang, Y.J., Yamamoto, A., Yamasu, K., Kuroiwa, A., et al., 2000. Zebrafish Mesp family genes, mesp-a and mesp-b are segmentally expressed in the presomitic mesoderm, and Mesp-b confers the anterior identity to the developing somites. Development 127, 1691–1702.

Sawada, A., Shinya, M., Jiang, Y.J., Kawakami, A., Kuroiwa, A., Takeda, H., 2001. Fgf/MAPK signaling is a crucial positional cue in somite boundary formation. Development 128, 4873–4880.

Serth, K., Schuster-Gossler, K., Cordes, R., Gossler, A., 2003. Transcriptional oscillation of lunatic fringe is essential for somitogenesis. Genes Dev. 17, 912–925.

Sieger, D., Tautz, D., Gajewski, M., 2003. The role of Suppressor of Hairless in Notch mediated signaling during zebrafish somitogenesis. Mech. Dev. 120, 1083–1094.

Tremblay, P., Dietrich, S., Mericskay, M., Schubert, F.R., Li, Z., Paulin, D., 1998. A crucial role for Pax3 in the development of the hypaxial musculature and the long-range migration of muscle precursors. Dev. Biol. 203, 49–61.

Winkler, C., Schäfer, M., Duschl, J., Schartl, M., Volff, J.-N., 2003a. Functional divergence of two zebrafish midkine growth factors following fish-specific gene duplication. Genome Res. 13, 1067–1081.

Winkler, C., Elmasri, H., Klamt, B., Volff, J.N., Gessler, M., 2003b. Characterization of hey bHLH genes in teleost fish. Dev. Genes Evol. 213, 541–553.

Wittbrodt, J., Meyer, A., Schartl, M., 1998. More genes in fish? BioEssays 20, 511–515.

Yoo, K.W., Kim, C.H., Park, H.C., Kim, S.H., Kim, H.S., Hong, S.K., et al., 2003. Characterization and expression of a presomitic mesoderm-specific mespo gene in zebrafish. Dev. Genes Evol. 213, 203–206.